WAVES IN THE SUNSPOT PENUMBRA

H. M. ANTIA and S. M. CHITRE

Tata Institute of Fundamental Research, Homi Bhabha Road, Bombay 400 005, India

and

M. H. GOKHALE

Indian Institute of Astrophysics, Bangalore, India

(Received 28 February, 1978)

Abstract. The stability of a plane-parallel polytropic fluid layer in the presence of a uniform horizontal magnetic field is investigated to explore the possibility of identifying the running penumbral waves and the penumbral filaments with different types of instabilities.

1. Introduction

An outstanding feature of any theory of sunspots is the role played by the spot magnetic field in influencing the mode of energy transport. It is now generally accepted that modified convection in some form must take place in a spot region, as there are convincing reasons to believe that sunspots cannot be in a completely radiative equilibrium (e.g. Chitre, 1963; Deinzer, 1965; Yun, 1970). The role of thermal dissipation in producing convective overstability was studied by Chandrasekhar (1952) in an attempt to investigate the convective transfer of heat under a constraint. His theory predicted the possibility that in the presence of a magnetic field instability can occur in the form of growing oscillations (overstability). Danielson (1961) employed Chandrasekhar's linearized equations to study the structure of the sunspot penumbra to demonstrate that instability in the penumbra will manifest as convection rolls if the penumbral magnetic field is assumed to be nearly horizontal and suggested that these rolls could account for the observed properties of the penumbral filaments.

The foregoing investigations were undertaken in the framework of the Boussinesq approximation which is applicable only when the thickness of the layer under consideration is much smaller than the scale height of any thermodynamic variable. Moreover in this approximation the acoustic modes which directly result from the effect of compressibility are filtered out. Moore and Spiegel (1966) have argued that the presence of thermal conduction could overstabilize the acoustic modes. It has been shown by Ando and Osaki (1975, 1977) that the observed five-minute oscillations on the solar surface are due mainly to the κ-mechanism operating in the hydrogen ionization zone. Antia *et al.* (1978, hereafter referred to as Paper I) studied the over-stabilization of acoustic modes in a polytropic atmosphere and found that acoustic modes can be overstabilized under suitable circumstances, even in the absence of κ-mechanism.

Solar Physics **60** (1978) 31–46.

The foregoing investigations are restricted to a non-magnetic fluid. The presence of the magnetic field gives rise to anisotropy in the fluid medium as the gravitational field and the magnetic field, each introduce a preferred direction. In addition the disturbances are subject to the combined effect of the three restoring forces arising from compressibility, buoyancy and magnetic field, and so the various pure modes (acoustic, gravity, and Alfvén) are severly modified. The problem of magneto-acoustic waves has been studied by a number of authors by adopting one of the following approaches. The first approach is based on neglecting the effect of zero-order stratification by assuming the unperturbed physical quantities to be constant over the fluid layer (Kato, 1966; Nakagawa *et al.*, 1973). This assumption can be justified only if the vertical extent of the fluid layer is much less than all the scale heights for variations of the physical quantities involved. The second approach is to investigate the stability of an isothermal atmosphere in which the sound speed, Alfvén velocity and density scale height are all taken constant by assuming the horizontal magnetic field to decrease exponentially with height. The dispersion relation for this case has been studied by Yu (1965) and more recently by Rudraiah *et al.* (1977). These models although not very realistic, nevertheless help us in understanding the variety of modes in a more complicated problem, and we have used them as guidelines for classifying the various modes.

Observationally, the penumbra consists of long filamentary structures (penumbral filaments) of thickness 300 km and length 2000 km arranged radially around the umbra. The characteristic life-time of a penumbral filament is 30 min (Danielson, 1961; Bray and Loughead, 1964). Besides these intensity inhomogeneities, recent observations have detected an interesting spectrum of velocity fields in the sunspots. The most remarkable pattern among these oscillations is the running penumbral waves discovered by Zirin and Stein (1972) and Giovanelli (1972), which propagate radially outward in sunspot penumbra, with predominantly vertical motions observed in Hα. Giovanelli (1974) has summarized the observational results of running penumbral waves which have periods in the range 180–240 s and horizontal wavelengths in the range of 2350–3800 km, and they travel outward in the penumbra at a typical speed of 15 km s^{-1}.

Nye and Thomas (1974, hereafter referred to as NT) have made a theoretical study of penumbral waves on the basis of a piecewise linear model of the vertical structure of a typical sunspot penumbra. They have identified the penumbral waves with magneto-acoustic fast ('plus'-type) waves, that are vertically trapped at photospheric levels, and have argued that the slow ('minus'-type) waves cannot be similarly trapped. However, their analysis overlooks the singularity in the governing differential equations. We have shown that if the singularity is properly considered, then it turns out that the slow modes can also be trapped, although our study supports their main conclusion that the penumbral waves can be identified with fast modes. In a later paper Nye and Thomas (1976) have studied the mode of running penumbral waves in a simpler but mathematically consistent two-layer penumbral model consisting of an upper isothermal layer with uniform horizontal magnetic field and a

lower adiabatic layer with a constant temperature gradient to find that observed frequencies and wavelengths of penumbral waves agree with those of the lowest fast mode.

The object of this paper is to study the stability of a plane parallel polytropic fluid layer with infinite electrical conductivity and finite radiative conductivity in the presence of a uniform horizontal magnetic field. We explore the possibility of identifying the running penumbral waves and the penumbral filaments with two different kinds of instabilities. For a reasonable choice of physical parameters we find that the time-scales and wave-lengths of fast modes for the disturbances propagating along the field lines roughly correspond to the observed values for the running penumbral waves.

2. Formulation of the Problem

We investigate the linear stability of a plane-parallel superadiabatic inviscid fluid layer in the presence of a uniform horizontal magnetic field. The governing hydrodynamical equations in the usual notation are:

momentum:

$$\rho\left(\frac{\partial \mathbf{v}}{\partial t}+\mathbf{v}\cdot\operatorname{grad}\mathbf{v}\right)=-\operatorname{grad}(P)+\rho\mathbf{g}+\frac{\mathbf{j}\times\mathbf{B}}{c},$$

continuity:

$$\frac{\partial \rho}{\partial t}+\operatorname{div}(\rho\mathbf{v})=0, \tag{1}$$

energy:

$$\rho C_v\left(\frac{\partial T}{\partial t}+\mathbf{v}\cdot\operatorname{grad}T\right)-RT\left(\frac{\partial \rho}{\partial t}+\mathbf{v}\cdot\operatorname{grad}\rho\right)=\operatorname{div}(K\operatorname{grad}T),$$

state:

$$P=R\rho T.$$

Here we assume the gas constant R and the specific heat at constant volume C_v to be constants thus neglecting any changes in the degree of ionization.

These equations are supplemented by Maxwell's equations

$$\begin{aligned}\operatorname{curl}\mathbf{H}&=\frac{4\pi}{c}\mathbf{j},\\ \operatorname{curl}\mathbf{E}&=-\frac{1}{c}\frac{\partial \mathbf{B}}{\partial t},\\ \operatorname{div}\mathbf{B}&=0.\end{aligned} \tag{2}$$

Introducing the further assumption that the fluid is ideally conducting we have

$$\mathbf{E}+\frac{\mathbf{v}\times\mathbf{B}}{c}=0\,. \tag{3}$$

Following Jones (1976) we have included the κ-mechanism by taking opacity x to be variable and assuming it to be of the form $x\sim\rho^{\lambda}T^{-\nu}$, where λ and ν are assumed to be constants. Then the thermal conductivity K is given by

$$K=\frac{4acT^3}{3x\rho}\sim\rho^{-\lambda-1}T^{3+\nu}\,. \tag{4}$$

We consider a polytropic fluid layer confined between two parallel horizontal planes at $z=0$ and $z=d$, which is stratified under constant gravity acting in the negative z-direction. If $T_{\rm base}$ and $T_{\rm top}$ are the temperatures at the lower and the upper boundaries respectively and $\rho_{\rm base}$ is the density at the lower boundary, then $T_r=T_{\rm top}/T_{\rm base}$ essentially determines the layer thickness d. Further for a uniform magnetic field the Lorentz force would vanish in the static state and this state would be the same as the corresponding non-magnetic case. Thus if

$$\Gamma=\frac{\mathrm{d}\ln P_0}{\mathrm{d}\ln\rho_0}=\frac{m+1}{m}$$

is the polytropic index, then in the undisturbed state $\rho_0\sim T_0^m$, $P_0\sim T_0^{m+1}$ where we have used the subscript zero to denote the various quantities in the static state. Now for the basic state to be polytropic we must demand the thermal conductivity K to be constant, i.e.

$$m(\lambda+1)=\nu+3\,. \tag{5}$$

This gives $x_0\sim T_0^{3-m}$ and the basic state turns out to be completely independent of the choice of λ or ν as long as Equation (5) is satisfied. For $\lambda=-1(\nu=-3)$ the perturbation terms arising from the variation of K will vanish and we can say that κ-mechanism will not be operative. A departure of λ from -1 will give rise to κ-mechanism and the value of $(\lambda+1)$ will control the effectiveness of the κ-mechanism. We have chosen two values of λ namely -1 and 3 for illustrating the numerical calculations.

We shall non-dimensionalize all the physical quantities with respect to the scale height $H=(RT_{\rm base}/g)$, the sound travel time $\sqrt{RT_{\rm base}}/g$, the pressure and temperature at the base of the layer. The unperturbed temperature is then given by $T=1-(1-(1/\Gamma))z$. Denoting the perturbed quantities by subscript one, we linearize the governing equations by writing all physical quantities in the form $f(z)=f_0(z)+f_1(z)\exp(\omega t+ik_xx+ik_yy)$, where k_x and k_y are the x and y components of the dimensionless horizontal wave number, and ω is the dimensionless eigenvalue which can be complex. In what follows we shall treat thermal

dissipation in the optically thick approximation. After a certain amount of elimination, the equations can be written in the following form:

$$
\begin{aligned}
&-\omega k_y P_1 + (\omega^2 \rho_0 + G_B k^2)(iv_y) + k_y G_B \frac{\mathrm{d}v_z}{\mathrm{d}z} = 0\,, \\
&\frac{\omega}{\Gamma T_0} v_z + \frac{\omega^2}{T_0}\theta - \left(\frac{\omega^2}{T_0} + k_x^2\right)\frac{P_1}{\rho_0} - \omega k_y (iv_y) - \omega \frac{\mathrm{d}v_z}{\mathrm{d}z} = 0\,, \\
&\omega \frac{\mathrm{d}P_1}{\mathrm{d}z} - G_B k_y \frac{\mathrm{d}(iv_y)}{\mathrm{d}z} - G_B \frac{\mathrm{d}^2 v_z}{\mathrm{d}z^2} = -(\omega^2 \rho_0 + G_B k_x^2) v_z + \\
&\qquad\qquad + \frac{\omega \rho_0}{T_0}\theta - \frac{\omega}{T_0} P_1\,, \\
&G_k\left[\frac{\mathrm{d}^2\theta}{\mathrm{d}z^2} - k^2\theta + (\lambda+1)\left(\frac{\omega T_0'}{T_0} v_z - \frac{1}{T_0}\frac{\mathrm{d}\theta}{\mathrm{d}z}\right)\right] = \\
&\qquad = -\left(1 - \frac{\gamma}{\Gamma}\right)\rho_0 v_z + \omega\gamma\rho_0\theta - \omega(\gamma-1)P_1\,.
\end{aligned}
\tag{6}
$$

Here p_1, ρ_1, θ are the perturbations in the pressure, density and temperature respectively, v_y and v_z are the components of velocity $\mathbf{v}$ in y and z directions, $k^2 = k_x^2 + k_y^2$, γ is the ratio of specific heats, G_k is the conductivity parameter,

$$
\frac{K_0 g}{\rho_{\text{base}} C_v (R T_{\text{base}})^{3/2}} = \frac{\kappa_0(0) g}{(R T_{\text{base}})^{3/2}}\,,
$$

where $\kappa_0 = K_0/(\rho_0 C_v)$ is the radiative diffusivity, G_B is the magnetic field parameter, $B_0^2/(4\pi R T_{\text{base}} \rho_{\text{base}})$ which is just the square of dimensionless Alfvén velocity at the lower boundary.

These equations have to be supplemented by boundary conditions at the upper and lower boundaries of the layer. We have used the following two sets of boundary conditions.

(a) Fixed boundary conditions in which both boundaries are maintained at constant temperature and there is no momentum flux across the boundaries:

$$
\rho_0 v_z = 0 \quad \text{and} \quad \theta = 0 \quad \text{at} \quad z = 0 \quad \text{and} \quad z = d\,.
$$

(b) Free boundary conditions at the upper boundary which demands the vanishing of Lagrangian pressure perturbations and the linearization of the radiative flux condition, and fixed boundary condition at the lower boundary of the layer:

$$
\left.
\begin{aligned}
&\rho_0 v_z - \omega P_1 + G_B \frac{\mathrm{d}v_z}{\mathrm{d}z} + G_B k_y (iv_y) = 0 \\
&\theta - \frac{\Gamma - 1}{\omega\Gamma} v_z + \frac{\Gamma T_0}{4(\Gamma-1)}\frac{\mathrm{d}\theta}{\mathrm{d}z} = 0
\end{aligned}
\right\} \quad \text{at} \quad z = d\,.
$$

It may be noted that the free boundary conditions are modified by the presence of magnetic field, since perturbations in the magnetic pressure also need to be considered.

The set of Equation (6) which is free from any singular coefficients was found to be suitable for numerical solution by the method discussed in Paper I. However by eliminating v_y from these equations, it can be reduced to a form similar to the non-magnetic equations of Paper I to get

$$\left(1-\frac{G_B k_y^2}{\omega^2\rho_0+G_B k^2}\right)\frac{\mathrm{d}v_z}{\mathrm{d}z}=$$

$$=\frac{1}{\Gamma T_0}v_z+\frac{\omega}{T_0}\theta-\left(\frac{\omega}{\rho_0 T_0}+\frac{k_x^2}{\omega\rho_0}+\frac{\omega k_y^2}{\omega^2\rho_0+G_B k^2}\right)P_1\,,$$

$$\left(1+\frac{G_B}{\rho_0 T_0}+\frac{G_B k_x^2}{\omega^2\rho_0}\right)\frac{\mathrm{d}P_1}{\mathrm{d}z}=$$

$$=-\left[\omega\rho_0+\frac{G_B k_x^2}{\omega}-\frac{G_B}{\omega\Gamma T_0^2}-\frac{G_B^2 k_y^2}{\omega\Gamma^2 T_0^2(\omega^2\rho_0+G_B k_x^2)}\right]v_z+$$

$$+\left[\frac{\rho_0}{T_0}+\frac{G_B}{T_0^2}+\frac{G_B^2 k_y^2}{\Gamma T_0^2(\omega^2\rho_0+G_B k_x^2)}\right]\theta- \tag{7}$$

$$-\left[\frac{1}{T_0}+\frac{G_B}{\rho_0 T_0^2}\left(1+\frac{1}{\Gamma}\right)+\frac{G_B(k^2+k_x^2)}{\omega^2\Gamma\rho_0 T_0}+\frac{G_B^2 k_y^2}{\Gamma T_0^2\rho_0(\omega^2\rho_0+G_B k_x^2)}\right]P_1+$$

$$+\frac{G_B}{T_0}\frac{\mathrm{d}\theta}{\mathrm{d}z}\,,$$

$$G_k\left[\frac{\mathrm{d}^2\theta}{\mathrm{d}z^2}-k^2\theta+(\lambda+1)\left(\frac{\omega T_0'}{T_0}v_z-\frac{1}{T_0}\frac{\mathrm{d}\theta}{\mathrm{d}z}\right)\right]=$$

$$=-\left(1-\frac{\gamma}{\Gamma}\right)\rho_0 v_z+\omega\gamma\rho_0\theta-\omega(\gamma-1)P_1\,.$$

It is evident that for $G_B=0$ and $\lambda=-1$, these equations are identical to corresponding equations of Paper I. We first consider the disturbances propagating along the lines of force i.e. ($k_y=0$). It is clear that in this case the equations have a singularity at the point given by

$$-\omega^2=\frac{G_B k_x^2/\rho_0}{1+(G_B/\rho_0 T_0)}=\frac{c_s^2 v_a^2 k_x^2}{c_s^2+\gamma v_a^2}\,, \tag{8}$$

where v_a is the Alfvén speed and c_s is the sound speed. Equation (8) can be evidently satisfied only for purely imaginary values of ω.

This singularity gives rise to the critical level phenomenon similar to that obtained for plane shear flow (cf. Booker and Bretherton, 1967). In a recent paper Adam (1977) has studied the significance of critical levels in the presence of magnetic fields. He found that waves are captured as they approach the critical level from either side

and are neither reflected nor transmitted but constrained to propagate along the field lines. The function on the right hand side of Equation (8) has a maximum at a point given by

$$T_0^{m+1} = \frac{G_B}{m} \quad \text{and} \quad -\omega_{\max}^2 = \frac{m}{m+1}\left(\frac{G_B}{m}\right)^{1/(m+1)} k_x^2.$$

Thus for $|\omega| > |\omega_{\max}|$ no such critical levels exist and the equation is free from singularities. This is the case for the fast modes which are unaffected by these critical levels. For purely imaginary values of ω such that $|\omega| < |\omega_{\max}|$ in general there can be two critical levels, but one or both of them may actually fall outside the layer under consideration. The frequencies of slow modes fall in the range of critical levels and as a result these levels put stringent restrictions on the slow modes that can be admitted by the boundary conditions and continuity requirements. It would thus appear that only a limited number of slow modes can exist. In the absence of dissipation ($G_k = 0$) we can eliminate θ by using the second equation in (7) and in that case the singularity will occur at

$$\omega^2 = -\frac{c_s^2 v_a^2 k_x^2}{c_s^2 + v_a^2}.$$

It then follows that the adiabatic equations of NT also have a singularity as can be clearly seen from the coefficient of k_z^2 in the dispersion relation (Equation (15) of NT). Thus at the point where $(c_s^2 + v_a^2)\omega^2 = c_s^2 v_a^2 k_x^2$, k_z^2 will be infinite. Further as we cross the singularity line

$$\omega = \left(\frac{c_s v_a}{\sqrt{c_s^2 + v_a^2}}\right) k_x$$

in the diagnostic diagram, k_z^2 will change from $+\infty$ to $-\infty$ or vice versa. As a result the waves would be propagating above the ω_+ curve in the form of fast modes as noted by NT (Figure 1), while the slow modes would be propagating between the singularity line and the ω_- curve instead of below the ω_- curve as conjectured by Nye and Thomas. This severely restricts the propagating region for slow modes in the diagnostic diagram and in fact it can be readily seen that the conclusion reached by NT that slow modes cannot be trapped in the photospheric layer is reversed. Figure 3 of NT should therefore be replaced by Figure 1 of the present paper, where the lines $2s$ and $3s$ represent respectively the singularity lines in the layers 2 and 3 of NT (the same set of parameters is used for comparing the figures). There is no magnetic field in layer 1 and hence the singularity line would coincide with the k_x-axis ($\omega = 0$). Also, since layer 1 is convectively unstable, the *-ve* mode curve has vanished. It can be clearly seen that almost all the slow modes which are propagating in layer 2 are evanescent in layers 1 and 3. Thus the slow modes can also be trapped in the photosphere.

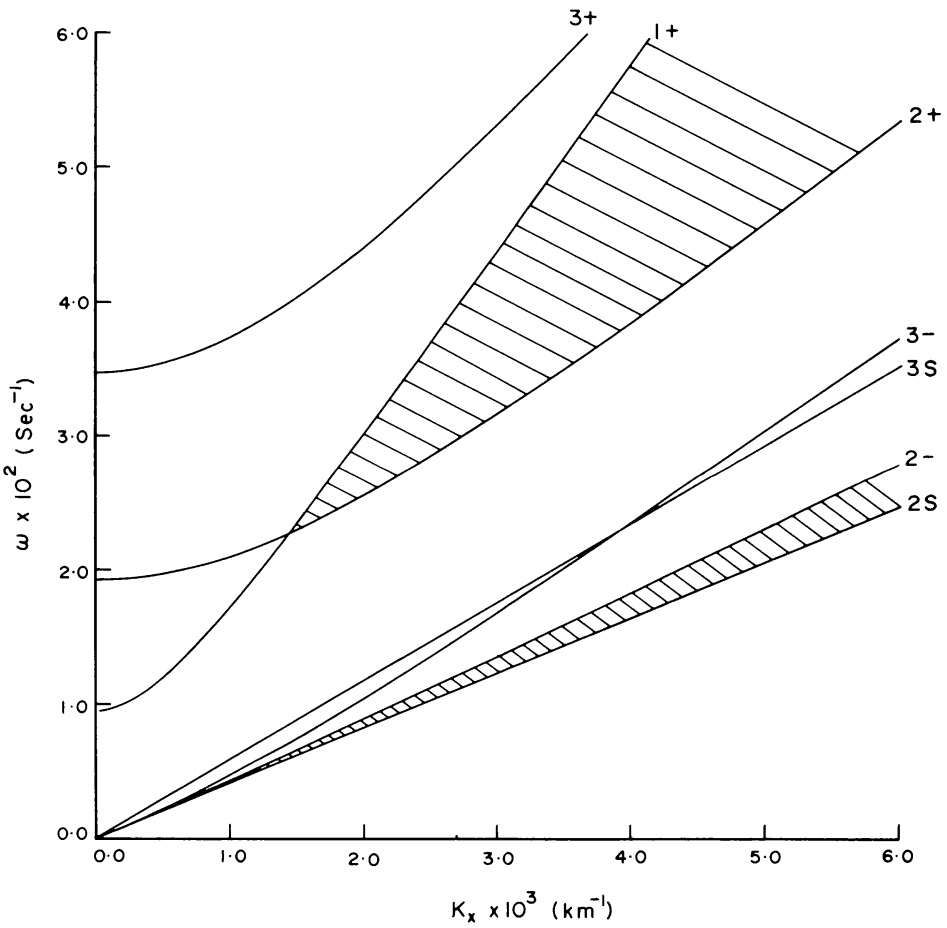

Fig. 1. The diagnostic diagram for values of c_s^2, v_a^2 and the scale height corresponding to three different levels of the penumbral model considered by NT. The shaded region indicates vertical trapping of fast and slow modes.

It may be noted that the critical levels will be absent for disturbances propagating perpendicular to the magnetic field lines (i.e. $k_x = 0$). For disturbances propagating in an arbitrary direction the situation will be more complex and we will not consider that case in the present analysis.

3. Modes with Wave Vector along the Magnetic Field Lines ($k_y = 0$)

We set $k_y = 0$ in Equation (6) to get $v_y \equiv 0$ and the motion in the horizontal plane is then restricted along the lines of force, while the vertical motion will always be perpendicular to the lines of force. The magnetic field provides an additional restoring force and as a result the frequencies of oscillatory modes will increase with the magnetic field strength. However the convective modes which give rise to steady circulation perpendicular to the field lines will tend to be stabilized. In general the various modes can be classified into three different categories: the fast and slow are oscillatory modes, while the convective modes have real eigenvalues. It may be noted that the Alfvén mode cannot arise if the Alfvén velocity varies with height. The

lowest fast mode (F-mode) has no nodes in pressure or velocity perturbations and the number of nodes in pressure perturbation increases with $|\omega|$. The successively higher modes will be denoted by P1, P2, P3, ... The fast mode tends to the usual acoustic modes in the limit of zero magnetic field and these are thus the acoustic modes modified by the magnetic field. The slow modes are oscillatory with much lower frequencies and as the magnetic field decreases, these modes tend to the convective or gravity modes. The convective modes have real eigenvalues and can be easily distinguished from the other two modes. The highest convective mode (F-mode) has no node in v_z and one node in P1.

We have solved Equation (6) numerically in order to compute the various eigenvalues ω for certain typical values of the parameters Γ, γ, G_k, G_B, λ, T_r and k_x. However because of the very large number of parameters involved in the present problem it is not possible to cover all the possible combinations and only a small representative set of values appropriate to the solar atmosphere was chosen. We choose $g = 2.47 \times 10^4$ cm s^{-2}, $T_{\text{base}} = 15\,000$ K and $\rho_{\text{base}} = 2.67 \times 10^{-6}$ g cm^{-3} to get a time scale of 45.2 s and a length scale of 504.9 km. We have selected three values of G_k namely 8.8×10^{-5}, 1.77×10^{-3} and 3.55×10^{-2} corresponding to the radiative diffusivity of 5×10^9, 10^{11}, and 2×10^{12} cm^{-2} s^{-1} respectively. For the magnetic field B we have assigned values 1000 G and 500 G, which typically represent the value of the horizontal component of the magnetic field near the inner boundary and in the middle regions of the penumbra (cf. Gokhale and Zwaan, 1972).

(a) *Fast Modes:* We find the frequency (imaginary part of ω) to increase with the magnetic field which is to be expected. Further the growth rates (real part of ω) are always quite small for small values of conductivity parameter and they are found to be rather sensitive to the choice of various parameters.

In the absence of the κ-mechanism ($\lambda = -1$) the magnetic field tends to stabilize the fast modes. As expected the κ-mechanism always tends to overstabilize the fast modes. For a value $\lambda = 3$ many of the modes which are stable for $\lambda = -1$ acquire positive growth rates. We summarise in Table I the complex eigenvalues of the first four fast modes for $\Gamma = 1.66$, $\gamma = 1.1$, $G_k = 0.0355$ and 0.001 77, $G_B = 0.0239$, 0.005 97 and 0.0, $\lambda = 3$, $T_r = 0.33$ and $k_x = 0$, 1, 2. For a value of the magnetic field $B = 1000$ G ($G_B = 0.0239$) appropriate to the sunspot penumbra, several of the modes are found to be overstable. For any given set of parameters in general, P1 and P2 modes have maximum growth rates which decrease with increasing k_x. This decrease is very mild for $k_x \lesssim 1$ and so we believe that it is of no consequence in determining the preferred wavelength of fast modes. It should be noted that $k_x = 1$ gives a wavelength $\approx$3200 km which is in the range of observed values for the running penumbral waves (Giovanelli, 1974). For different choices of parameters the frequency of the most unstable mode is in the range of 1.4 to 3.3 which gives time scales in the range 85 to 200 s. This is somewhat less than the observed range of 180 to 240 s. Further the phase velocity of these wave modes is of order of 15–40 km s^{-1}.

In all cases it has been found that the lowest fast mode (F-mode) is damped and so it is unlikely to be observed. Thus the running penumbral waves should be identified

TABLE I

Real and imaginary parts of eigenvalues of the first four harmonics of acoustic modes for $\Gamma = 1.66$, $\gamma = 1.1$, $T_r = 0.33$, $k_y = 0.0$, $\lambda = 3$, for different values of G_B, G_k, and k_x. The numbers in parenthesis are the powers of ten.

k_x	Mode	$G_B = 0.0$				$G_B = 0.005\,97$				$G_B = 0.0239$			
		$G_k = 0.001\,77$		$G_k = 0.0355$		$G_k = 0.001\,77$		$G_k = 0.0355$		$G_k = 0.001\,77$		$G_k = 0.0355$	
0.0	P1	1.49(−3)	1.582	5.50(−3)	1.605	1.71(−3)	1.601	6.68(−3)	1.625	2.12(−3)	1.655	9.81(−3)	1.681
	P2	−2.13(−3)	3.094	8.96(−3)	3.094	−1.65(−3)	3.134	1.02(−2)	3.136	−6.69(−4)	3.246	1.38(−2)	3.253
	P3	−7.21(−3)	4.621	1.21(−3)	4.587	−6.45(−3)	4.682	1.79(−3)	4.651	−4.82(−3)	4.851	4.28(−3)	4.827
	P4	−1.36(−2)	6.153	−1.44(−2)	6.082	−1.25(−2)	6.234	−1.44(−2)	6.167	−1.01(−2)	6.459	−1.32(−2)	6.402
1.0	F	−1.45(−3)	0.909	−1.51(−2)	0.906	−1.44(−3)	0.910	−1.52(−2)	0.907	−1.41(−3)	0.911	−1.52(−2)	0.909
	P1	7.37(−4)	1.796	7.68(−3)	1.818	9.99(−4)	1.814	9.00(−3)	1.837	1.55(−3)	1.864	1.25(−2)	1.889
	P2	−2.55(−3)	3.206	6.87(−3)	3.205	−2.05(−3)	3.245	8.22(−3)	3.246	−1.00(−3)	3.355	1.21(−2)	3.361
	P3	−7.53(−3)	4.697	−1.19(−3)	4.661	−6.75(−3)	4.756	−5.33(−4)	4.724	−5.09(−3)	4.924	2.12(−3)	4.899
2.0	F	−5.42(−4)	1.768	8.03(−4)	1.776	−4.83(−4)	1.771	5.85(−4)	1.779	−3.80(−4)	1.779	−8.74(−5)	1.788
	P1	−1.70(−3)	2.325	1.15(−4)	2.336	−1.36(−3)	2.339	1.86(−3)	2.352	−5.59(−4)	2.383	6.72(−3)	2.399
	P2	−3.80(−3)	3.521	−3.86(−5)	3.516	−3.25(−3)	3.557	1.52(−3)	3.555	−2.03(−3)	3.662	6.08(−3)	3.665
	P3	−8.48(−3)	4.916	−8.27(−3)	4.877	−7.67(−3)	4.973	−7.43(−3)	4.938	−5.89(−3)	5.137	−4.36(−3)	5.109

with P1 or P2 modes which turn out to be the most unstable modes. Another curious result is that for $\lambda = 3$ the magnetic field tends to destabilize the modes in contrast to the stabilizing effect for $\lambda = -1$. Thus it appears that the κ-mechanism is essential for driving of oscillations in the presence of a horizontal magnetic field.

The foregoing results are obtained for fixed boundary conditions which are of course not realistic when applied to the solar surface layers. To get somewhat nearer to reality, we have considered free boundary conditions, for which most of the modes turn out to be stable in the absence of the κ-mechanism. Even for $\lambda = 3$ the magnetic field tends to stabilize the fast modes. However for field strength of 1000 G ($G_B = 0.0239$) and for highest chosen value of G_k (0.0355) the free boundary conditions tend to give growth rates larger by a factor of 2 to 3 for the fast modes compared to those for rigid boundaries. Further the maximum growth rate is now attained for P3 modes which have frequency ≈ 4 corresponding to a time scale ≈ 70 s. In this case also the maximum growth rate decreases with k_x although for $k_x \lesssim 1$ the decrease is not very pronounced to be of any consequence in determining a preferred wavelength. For lower values of G_k the free boundary condition tend to stabilize the fast modes. Thus we see that the maximum growth rates are obtained for periods which are two times lower than the observed values. It may be noted that the growth rates are somewhat sensitive to various parameters and so for a realistic model of the solar penumbra the maximum growth rates may be obtained at lower harmonics which could yield periods in the range of the observed values.

(b) *Slow Modes:* It has been noted earlier that the slow modes are controlled by the critical levels in the fluid layer. Numerically it was found rather difficult to compute the eigenvalues of these modes and so only a few of the slow modes are calculated to find that the κ-mechanism tends to stabilize them. For $\Gamma = 1.33$, $\gamma = 1.1$, $G_k = 0.0355$, $G_B = 0.0239$, $\lambda = 3$, $T_r = 0.33$, and $k_x = 1$, with rigid boundary condition, the only slow mode calculated has the eigenvalue $0.033 + 0.168i$, while for $\lambda = -1$ it has the eigenvalue $0.052 + 0.147i$. Thus it can be seen that the growth rate of this mode is roughly two times that of the most unstable fast mode for the same choice of the basic parameters. This mode gives a time period ≈ 1700 s and it seems highly unlikely that the running penumbral waves have any relationship with the slow modes. Another reason for not identifying the penumbral waves with the slow modes is that the frequency and growth rate of the slow mode is very sensitive to the choice of the basic parameters especially the magnetic field while the penumbral waves which have been observed in practically all the sunspots have a very narrow range of periods and associated wavelengths. Also the slow modes are not sensitive to the boundary conditions and for the same set of parameters but with more realistic free boundary conditions the slow mode has eigenvalue $0.036 + 0.166i$, while the growth rate of the fastest growing fast mode (P3 mode) is 0.041. Thus it appears that with more realistic boundary conditions the fast modes grow faster than the slow modes. Observationally it may be rather difficult to detect the slow modes though their growth rates seem to be comparable to those of the fastest growing fast modes.

(c) *Convective Mode:* In the absence of the magnetic field and thermal dissipation, the convective modes can appear if the temperature gradient is superadiabatic (i.e. $\Gamma > \gamma$). But in the presence of magnetic field this condition is modified and if the coefficients in the Equation (6) (with $G_k = 0$) are assumed to be locally constant this can be written as

$$1 - \frac{\gamma}{\Gamma} > \frac{G_B \gamma T_0}{\rho_0} (k_x^2 + k_z^2), \tag{9}$$

where k_z is the local vertical wavenumber. The unique feature of this condition which distinguishes the magnetic case from the non-magnetic case is the occurrence of $(k_x^2 + k_z^2)$ in the right hand side of the inequality. Thus for sufficiently large value of k_x or k_z (i.e. sufficiently higher order modes) this condition can always be violated for any finite non-zero value of G_B. Thus for large values of k_x or G_B there will be no convective modes. For a small value of k_x only a finite number of convective modes exist, while the higher modes will manifest themselves as slow modes. This is in contrast to the possibly denumerably infinite number of convective modes in the absence of magnetic field. In this manner, as G_B increases, large number of convective modes will go over into the slow modes. It should however be noted that the number of slow modes is strictly controlled by the critical levels in the layer, and it is not altogether clear whether the spectrum of slow modes is finite or infinite. This is especially true in the presence of dissipation, when the eigenvalues can have a non-zero real part and there is no singularity in the governing equations. An interesting feature of condition (9) is that the convective modes for higher k_x are damped more pronouncedly by the magnetic field. Consequently the growth rates for convective modes posses a distinct maximum for some value of k_x which otherwise they would not. This gives rise to a preferred scale of convective modes even in the absence of dissipation.

The above conclusions are borne out by our numerical computations which show that for small values of G_B and k_x there is a limited number of convective modes. In Table II we give the real eigenvalues for the case $\Gamma = 1.33$ and 1.66, $G_k = 0.0$, 0.001 77 and 0.0355, $\gamma = 1.1$, $T_r = 0.33$, $\gamma = -1$, $k_x = 1, 2, 4, 6$, and $G_B = 5.97 \times 10^{-3}$ ($B = 500$ G). We find that the eigenvalues decrease as G_k increases and for the highest chosen value of G_k (0.0355) in most cases there are no growing convective modes. It is found that the magnetic field tends to stabilize the convective modes by decreasing the growth rates, a decrease which is more pronounced for higher values of k_x. Consequently the maximum growth rate occurs at lower values of k_x with the preferred length scale correspondingly larger; at the same time the maximum growth rate becomes smaller with the e-folding times correspondingly larger. We also find that the κ-mechanism tends to stabilize the convective modes although the effect is somewhat less pronounced and the growth rates for convective modes turn out to be insensitive to the boundary conditions. The e-folding times for the convective modes are in the range 100 to 400 s and these modes may not be

TABLE II

Eigenvalues of convective modes for $\gamma = 1.1$, $T_r = 0.33$, $G_B = 0.00597$, $\lambda = -1$, $k_y = 0.0$, for different values of Γ, G_k and k_x. For $\Gamma = 1.33$ and $G_k = 0.0355$ no growing convective mode was found. The numbers in parenthesis preceding the eigenvalues are the numbers of nodes in v_z, for the corresponding eigenfunctions.

k_x	$\Gamma = 1.33$		$\Gamma = 1.66$		
	$G_k = 0.0$	$G_k = 0.001\,77$	$G_k = 0.0$	$G_k = 0.001\,77$	$G_k = 0.0355$
1.0	(0) 0.2379	(0) 0.2276	(0) 0.2794	(0) 0.2702	(0) 0.1380
	(1) 0.1078	(0) 0.0024	(1) 0.1353	(1) 0.0895	(0) 0.0373
			(2) 0.0524	(1) 0.0300	
				(0) 0.0016	
2.0	(0) 0.2762	(0) 0.2520	(0) 0.4232	(0) 0.4067	
	(1) 0.1148	(0) 0.0138	(1) 0.2320	(1) 0.1697	
			(2) 0.0809	(1) 0.0470	
				(0) 0.0047	
4.0			(0) 0.4321	(0) 0.3679	
			(1) 0.2474	(0) 0.0472	
6.0			(0) 0.1627		

observable in the presence of the steady, Evershed flow. Moreover for higher values of G_k which are probably more appropriate for sunspot penumbra there are no convective modes present and so naturally they cannot be observed.

A remarkable feature in this case is the existence of another series of growing real modes in the presence of thermal dissipation. This may be attributed to the transformation of a pair of growing slow modes into a pair of growing convective modes. These modes are essentially the same as the usual convective modes but with a smaller value of ω and also have the property that the number of nodes in v_z decreases with ω. Thus the lowest mode has no node in v_z while the successively higher modes have one more node in v_z. These are the diffusive modes.

4. Modes with Wave Vector Perpendicular to Magnetic Field Lines ($k_x = 0$)

In this case it can be seen from the basic equations that the component of velocity along the magnetic field vanishes ($v_x \equiv 0$) and so the motion is always perpendicular to the lines of force. There will in general be three types of modes. The fast modes are essentially similar to those discussed for the case $k_y = 0$. The only interesting feature about the fast modes is that the growth rates are 3–4 times smaller than those for the corresponding modes for the case $k_y = 0$. These modes are therefore not expected to be observed in the sunspot penumbra. The slow modes are completely different in character because of the absence of critical levels in this case. In the absence of thermal dissipation if we treat the coefficients in Equation (6) as locally constant,

then it follows that the convective modes exist if

$$\Gamma - \gamma > \frac{G_B}{\rho_0 T_0}. \tag{10}$$

The essential difference between condition (10) and condition (9) is the absence of k_y and k_z. It would then appear that the perturbations with any wavenumber can be locally stable or unstable with respect to convection. Thus if $G_B > (\Gamma - \gamma)$, there will be no convective modes, and for $G_B/(\rho_0(d)T_0(d)) < (\Gamma - \gamma)$ there will be no oscillatory (slow) modes. For intermediate values of G_B a portion of the layer at the top will be stable with respect to the convective modes, while the lower portion would be convectively unstable. In this fashion the problem would be somewhat similar to the problem of two-fluid layer model with a stable upper layer overlying an unstable lower layer. And in general both the oscillatory (slow) and the convective modes can be expected to prevail in such a layer. Of course it must be noted that $\rho_0 \sim T_0^m$ and that ρ_0 occurs in the coefficients of Equation (6) and hence to treat them as locally constant can hardly be justified. Nevertheless this analysis helps to gain some insight into the classification of modes. Further it is also not clear from this analysis how thermal dissipation would affect the various modes.

It is found that for intermediate values of G_B both slow and convective modes can exist, and that in both cases the mode with highest value of $|\omega|$ has no node in v_z, while the number of nodes increases as $|\omega|$ decreases. In fact the calculated eigenfunctions show that the various perturbed quantities are very small in the upper portion of the layer for convective modes and in the lower portion of the layer for the slow modes. Thus the qualitative behaviour obtained on the basis of the locally constant coefficients is borne out. These convective modes may be identified with the convective rolls as discussed by Danielson (1961) while discussing the stability of a plane parallel layer in the framework of the Boussinesq approximation. In this case also there is a second series of growing convective modes in the presence of thermal dissipation presumably of diffusive origin.

The slow modes are again found to be difficult to compute numerically but some of the calculated modes turn out to be overstable with significant growth rates ≈ 0.01.

Convective Mode: The magnetic field tends to stabilize the convective modes with the growth rates decreasing with increasing magnetic field. The growth rates also decrease as G_k increases. As in the non-magnetic case, in the absence of dissipation the growth rates are a monotonically increasing function of k_y. But in the presence of thermal dissipation the growth rates attain a maximum value for some finite value of k_y, thus giving a preferred length scale for convection. The value of k_y for maximum growth rates decreases with increasing G_k. Consequently for higher G_k, the preferred length scale would be larger and at the same time the growth rates would be lower. The convective modes are not sensitive to boundary conditions and the κ-mechanism is found to have a mild stabilizing influence on them.

In Table III we summarize the convective modes for $\Gamma = 1.33$, $\gamma = 1.1$, $T_r = 0.33$, $G_k = 0.0355$, 0.00 177 and 0.0, $G_B = 0.0239$ and 0.00 597, $\lambda = -1$ and $k_y =$

TABLE III

Eigenvalues of convective modes for $\Gamma = 1.33$, $\gamma = 1.1$, $T_r = 0.33$, $\lambda = -1$, $k_x = 0.0$, for different values of G_B, G_k, and k_y. For $G_B = 0.0239$ and $G_k = 0.0355$ no growing convective mode was found. The numbers in parenthesis preceding the eigenvalues are the numbers of nodes in v_z for the corresponding eigenfunctions.

k_y	$G_B = 0.005\,97$			$G_B = 0.0239$	
	$G_k = 0.0$	$G_k = 0.001\,77$	$G_k = 0.035\,55$	$G_k = 0.0$	$G_k = 0.001\,77$
1.0	(0) 0.2490	(0) 0.2386	(0) 0.1182	(0) 0.1833	(0) 0.1733
	(1) 0.1531	(1) 0.1242	(0) 0.0180	(1) 0.0984	(1) 0.0587
	(2) 0.1059	(2) 0.0523		(2) 0.0653	(1) 0.0173
	(3) 0.0800	(2) 0.0076		(3) 0.0485	(0) 0.0035
2.0	(0) 0.3493	(0) 0.3293	(0) 0.1196	(0) 0.2694	(0) 0.2513
	(1) 0.2569	(1) 0.2162	(0) 0.0352	(1) 0.1744	(1) 0.1252
	(2) 0.1927	(2) 0.1252		(2) 0.1231	(1) 0.0193
	(3) 0.1512	(2) 0.0077		(3) 0.0938	(0) 0.0057
4.0	(0) 0.4063	(0) 0.3568		(0) 0.3291	(0) 0.2869
	(1) 0.3513	(1) 0.2788		(1) 0.2607	(1) 0.1774
	(2) 0.2987	(2) 0.1951		(2) 0.2068	(1) 0.0310
	(3) 0.2538	(3) 0.1110		(3) 0.1678	(0) 0.0121
6.0	(0) 0.4222	(0) 0.3382		(0) 0.3490	(0) 0.2753
	(1) 0.3861	(1) 0.2770		(1) 0.3012	(1) 0.1714
	(2) 0.3494	(2) 0.2055		(2) 0.2567	(1) 0.0497
	(3) 0.3134	(3) 0.1263		(3) 0.2194	(0) 0.0210
8.0	(0) 0.4293	(0) 0.3093		(0) 0.3582	(0) 0.2466
	(1) 0.4021	(1) 0.2544		(1) 0.3230	(0) 0.0330
	(2) 0.3757	(2) 0.1900		(2) 0.2872	
	(3) 0.3481	(3) 0.1137		(3) 0.2546	

1, 2, 4, 6, 8. It can be seen that for the choice $G_k = 1.77 \times 10^{-3}$ the maximum growth rate (≈ 0.3) is attained for k_y between 4 and 6. This gives a half wavelength of 250–400 km and e-folding time ≈ 2.5 min. This can be compared with length scale of 300 km and lifetime of 30–40 min for the penumbral filaments. Thus it can be seen that although the length scale agrees with the observed values, the e-folding time is more than an order of magnitude smaller as compared to observed lifetimes. However these results must be viewed with caution since the eigenvalues of convective modes are very sensitive to a number of parameters such as $(\Gamma - \gamma)$, G_k and by changing these parameters suitably we can get a very wide range of e-folding times and length scales.

It is found that as G_k increases or as $(\Gamma - \gamma)$ decreases the growth rates for the two series of convective modes approach each other and ultimately they merge together to give a pair of growing slow modes. This gives a lower limit on the growth rates of convective modes. The length scale of convection is essentially controlled by the conductivity parameter G_k. For $G_k = 8.8 \times 10^{-5}$ the length scale turns out to be $\lesssim 200$ km, while for $G_k = 1.77 \times 10^{-3}$ it is in the range of 200–400 km for still higher

value of G_k (0.0355) it is ≈800 km. The e-folding time for various set of values of parameters falls in the range of 1 min to 12 min.

The main conclusion from our computations of an idealized penumbral model is that the running penumbral waves could be identified with the fast magneto-acoustic modes propagating along a horizontal magnetic field in the sunspot penumbra. The time scales and the associated wavelengths come out to be in reasonable agreement with the corresponding observed values for the running penumbral waves. It should, however be stressed that the observed field across the penumbra is not strictly horizontal and in fact it varies by an order of magnitude from the inner edge of the penumbra to the outer edge of the spot. Nevertheless, our simplified model indicates the kind of modes excited at the photospheric levels that may be identified with the running penumbral waves.

The situation concerning the penumbral filaments is not all that clear. The convective modes arising from disturbances with wave vector perpendicular to the magnetic field lines have half wave-length of the order of the thickness of the long filamentary structures but their characteristic e-folding times come out to be an order of magnitude smaller than the lifetimes of the filaments. But it should be remarked that the growth rates of convective modes depend rather sensitively on a number of parameters including the degree of superadiabaticity, the inclination of wave vector to the magnetic field and the radiative conductivity. By suitably adjusting these parameters it is not altogether impossible to bring the e-folding times in accordance with the observed filamentary time-scales.

References

Adam, J. A.: 1977, *Solar Phys.* **52**, 293.
Ando, H. and Osaki Y.: 1975, *Publ. Astron. Soc. Japan* **27**, 581.
Ando, H. and Osaki Y.: 1977, *Publ. Astron. Soc. Japan* **29**, 221.
Antia, H. M., Chitre, S. M., and Kale, D. M.: 1978, *Solar Phys.* **56**, 275.
Booker, J. R. and Bretherton, F. P.: 1967, *J. Fluid Mech.* **27**, 513.
Bray, R. J. and Loughhead, R. E.: 1964, *Sunspots*, Chapman and Hall, London.
Chandrasekhar, S.: 1952, *Phil. Mag.* **43**, 501.
Chitre, S. M.: 1963, *Monthly Notices Roy. Astron. Soc.* **126**, 431.
Danielson, R. E.: 1961, *Astrophys. J.* **134**, 275.
Deinzer, W.: 1965, *Astrophys. J.* **141**, 548.
Giovanelli, R. G.: 1972, *Solar Phys.* **27**, 71.
Giovanelli, R. G.: 1974, in R. Grant Athay (ed.), 'Chromospheric Fine Structure', *IAU Symp.* **56**, 137.
Gokhale, M. H. and Zwaan, C.: 1972, *Solar Phys.* **26**, 52.
Jones, C. A.: 1976, *Monthly Notices Roy. Astron. Soc.* **176**, 145.
Kato, S.: 1966, *Publ. Astron. Soc. Japan* **18**, 201.
Moore, D. W. and Spiegel, E. A.: 1966, *Astrophys. J.* **143**, 871.
Nakagawa, Y., Priest, E. R., and Wellck, R. E.: 1973, *Astrophys. J.* **184**, 931.
Nye, A. H. and Thomas, J. H.: 1974, *Solar Phys.* **37**, 399.
Nye, A. H. and Thomas, J. H.: 1976, *Astrophys. J.* **204**, 582.
Rudraiah, N., Venkatchalappa, M., and Kandaswamy, P.: 1977, *J. Fluid Mech.* **80**, 223.
Yu, C. P.: 1965, *Phys. Fluid* **8**, 650.
Yun, H. S.: 1970, *Astrophys. J.* **162**, 975.
Zirin. H. and Stein, A.: 1972, *Astrophys. J.* **173**, 185.